






Article

A Cucumber AGAMOUS-LIKE 15 (AGL15) MADS-Box Gene Mediates Abnormal Leaf Morphology in *Arabidopsis*

Yong Zhou ^{1,2,+} , Lingli Ge ^{3,+} , Lifang Hu ^{2,3} , Yingui Yang ³  and Shiqiang Liu ^{1,*} ¹ College of Science, Jiangxi Agricultural University, Nanchang 330045, China; yzhouxau@163.com² Key Laboratory of Crop Physiology, Ecology and Genetic Breeding, Ministry of Education, Jiangxi Agricultural University, Nanchang 330045, China; lfhu_hn337@163.com³ College of Agronomy, Jiangxi Agricultural University, Nanchang 330045, China; gelingli0401@163.com (L.G.); yangyingui@163.com (Y.Y.)

* Correspondence: lsq_hn306@163.com; Tel.: +86-0791-83813574

+ These authors contributed equally to this work.

Received: 19 October 2018; Accepted: 13 November 2018; Published: 17 November 2018



Abstract: The AGL15 subfamily MADS-box proteins play vital roles in various developmental processes, such as floral transition, somatic embryogenesis, and leaf and fruit development. In this work, an *AtAGL15* ortholog, *CsMADS26*, was cloned from cucumber (*Cucumis sativus* L.). The open reading frame (ORF) of *CsMADS26* is 669 bp in length, encoding a predicted protein of 222 amino acids. The *CsMADS26* protein contains a highly conserved MADS-box domain and a variable C domain, as well as less conserved I and K domains. Phylogenetic relationship analysis revealed that *CsMADS26* was clustered into the AGL15 clade of AGL15 subfamily. Expression analysis based on qRT-PCR showed that *CsMADS26* is mainly expressed in reproductive organs including flowers and fruits. Transgenic *Arabidopsis* plants with ectopic expression of *CsMADS26* exhibited curled rosette and cauline leaves, and the leaf size was much smaller than that of wild-type (WT) plants. These results provide clues for the functional characterization of *CsMADS26* in the future.

Keywords: cucumber; MADS-box; AGAMOUS-LIKE 15 (AGL15); transgenic *Arabidopsis*; curled leaf; leaf size

1. Introduction

MADS intervening keratin-like and C-terminal (MIKC)-type MADS-box transcription factors (TFs) are a type of MADS-box proteins only present in plants, and are known for the four characteristic domains from N to C terminus: the highly conserved MADS domain (M); the poorly conserved intervening domain (I); the relatively conserved Keratin-like domain (K); and the most variable C-terminal domain (C) [1,2]. According to the structural divergence of I and K domains, MIKC-type MADS-box genes are further classified into two subgroups named as MIKC^C and MIKC* [3,4]. The MIKC^C-type is the MADS-box that has been most extensively studied in plants, and can be further divided into at least 13 subfamilies named after their first identified members, such as AGAMOUS (AG), SHORT VEGETATIVE PHASE (SVP), FLOWERING LOCUS C (FLC), APETALA1 (AP1), AP3, SUPPRESSOR OF OVEREXPRESSION OF CO1 (SOC1), SEPALLATA (SEP), AGAMOUS-LIKE 6 (AGL6), AGL12, AGL15, AGL17, TM8 (TOMATO MADS-box 8), and B_{sister} (BS) [5–8].

AGL15 and AGAMOUS-LIKE18 (AGL18) constitute the AGL15 subfamily, and many AGL15 subfamily members were recently identified by genome-wide approaches in many plant species, including *Cucumis melo* [6], *Pyrus bretschneideri* [9], *Ziziphus jujuba* [10], *Gossypium hirsutum* [2,11], *Dianthus caryophyllus* [12], *Morus notabilis* [7], and *Hevea brasiliensis* [13]. These studies showed

that the expression of AGL15 subfamily members is primarily detected in floral organs, implying their important roles in the development of floral organs. For example, *agl15 agl18* double mutants displayed an early flowering phenotype, which was not observed in *agl15* or *agl18* single mutants, suggesting that *AtAGL15* and *AtAGL18* act as co-repressors for floral transition [14]. Further studies showed that *AtAGL15* can interact with *AtAGL18* to form a complex with other proteins, which could directly bind to the promoters of *MIR156a/c* to activate the expression of *MIR156*, and delay the floral transition in *Arabidopsis* [15]. In addition to controlling floral transition, ectopic expression of *AtAGL15* or *AtAGL18* in *Arabidopsis* can also enhance somatic embryogenesis, affect leaf morphogenesis, reduce fertility, and delay floral organ senescence and abscission [14,16,17], indicating the redundant functions of *AtAGL15* and *AtAGL18* in these developmental processes. *AtAGL15* orthologs have been functionally characterized in other plants, such as cotton (*G. hirsutum*) [18], soybean (*Glycine max*) [19–21], *Rosa canina* [22], and *Brassica juncea* [23]. In addition, AGL15 members can control diverse developmental processes by modulating the hormone signaling pathways. For example, *AtAGL15* and *GmAGL15* negatively regulate auxin signaling pathway to promote somatic embryogenesis in *Arabidopsis* and soybean, and this regulation is integrated with GA metabolism and ethylene signaling pathway [19,20,24,25]. Overexpression of an *AtAGL15* ortholog from *R. canina* in *Arabidopsis* altered floral organ morphology and numbers, as well as somatic embryogenesis, with a reduction in IAA and GA contents [22].

Recently, several MADS-box members have been identified and functionally characterized in cucumber [26,27]. However, the biological function of *AtAGL15* orthologs in cucumber has not been elucidated. In this study, an AGL15 gene (*CsMADS26*) was isolated from cucumber based on the sequence of *Csa020302* available in our previous study [28]. To study the biological function of *CsMADS26*, we overexpressed this gene in *Arabidopsis* and examined the phenotypes of the transgenic plants. The findings may aid in further clarification of the biological function of *CsMADS26* in the growth and development of cucumber.

2. Materials and Methods

2.1. Plants and Growth Conditions

Cucumis sativus var. *sativus* line 9930 and *Arabidopsis* (Col-0) were used in this study. The cucumber seedlings were planted in the field of Jiangxi Agricultural University, Nanchang, China, under natural conditions. Wild-type (WT, Col-0) and transgenic *Arabidopsis* plants were planted in a growth room at 22 °C under long-day conditions (16 h of light/8 h of dark) with a relative humidity of 60%.

2.2. Isolation of the ORF of *CsMADS26*

To isolate *CsMADS26*, flower RNA extraction was performed using the Trizol reagent (TianGen, Beijing, China) according to the manufacturer's protocol. The concentrations of RNA were examined by using Nanodrop 2000 (Thermo Fisher Scientific, Wilmington, NC, USA) and the RNA integrity was verified by agarose gel electrophoresis. After removal of potential DNA contamination, the first-strand cDNA was synthesized by using the TransScript One-Step gDNA Removal and cDNA Synthesis SuperMix kit (TransGen, Beijing, China) from 3 µg of total RNA.

The specific primers (*CsMADS26*-1F: 5'-ATGGGTCGAGGGAAGATTGAAAT-3', and *CsMADS26*-1R: 5'-TTACCCCAAGTGCAAGGTGGTGT-3') used for *CsMADS26* gene (locus ID: *Csa020302*) were designed for amplifying the open reading frame (ORF) of *CsMADS26* using cucumber flower cDNA as the template. The reverse transcription polymerase chain reaction (RT-PCR) reaction procedure was as follows: 5 min initial denaturation at 95 °C, followed by 30 cycles at 95 °C for 1 min, 58 °C for 1 min, 72 °C for 1 min, and a final extension at 72 °C for 7 min. The amplified products were separated on 1.0% agarose gel and purified using a nucleic acid purification kit (Sangon, Shanghai, China). The resulting PCR products were ligated into the pMD18-T vector (TaKaRa, Dalian, China). The positive pMD18-*CsMADS26* clones were confirmed by PCR with the above-mentioned

primers (CsMADS26-1F and CsMADS26-1R), and then sequenced at Tsingke Biological Technology Company (Tsingke, Beijing, China).

2.3. Bioinformatics Analysis

The physicochemical and biochemical properties of CsMADS26 protein were analyzed using the programs of ExPASy ProtParam and SOPMA [29]. The prediction of subcellular localization for CsMADS26 protein was executed by WoLF PSORT (<https://www.genscript.com/tools/wolf-psort>). The online SMART server (<http://smart.embl-heidelberg.de>) was employed to analyze the conserved domains of CsMADS26 protein. Multiple alignments were carried out using Clustal Omega [30], by aligning the sequences of CsMADS26 and AGL15 subfamily proteins from different plants. Subsequently, a phylogenetic tree was created by the MEGA 5.0 software using the Neighbor-Joining (NJ) method with default settings, except that the bootstrap value was set at 1000 replicates.

2.4. Expression Analysis of the CsMADS26 Gene

To investigate the tissue expression profiles of CsMADS26, total RNA was prepared from six different tissues of *C. sativus* var. *sativus* line 9930, including male flower, female flower, root, stem, leaf, and fruit. The first-strand cDNA was synthesized as described above, and quantitative real-time PCR (qRT-PCR) was employed to determine the expression of CsMADS26 in these tissues by using *CsAct3* (5'-GGCAGTGGTGGTGAACAT-3', and 5'-GATTCTGGTGATGGTGTGAGTC-3') as the internal control. The CsMADS26-specific primers were as follows: CsMADS26-2F (5'-GCACAAGGTTGAGCGAGAG-3') and CsMADS26-2R (5'-TGAAGCCTAAGCCAGTGAGAT-3'). The qRT-PCR was conducted in triplicate on LightCycler 480 Real-Time PCR System with the SYBR Green I Master Mix (Roche), and the conditions were as follows: 95 °C for 30 s, followed by 40 cycles at 95 °C for 5 s, 60 °C for 30 s, and 72 °C for 15 s. The relative expression levels were calculated according to the $2^{-\Delta\Delta C_t}$ method [31].

2.5. Vector Construction and Genetic Transformation

The positive pMD18-CsMADS26 was digested with *Pst* I and *Xba* I, and ligated into the pHB vector to generate the 35S::35S::CsMADS26 construct, in which the ORF of CsMADS26 was under the control of a double 35S promoter, and the *hygromycin* gene was used as a selectable marker. The 35S::35S::CsMADS26 construct was introduced into *Agrobacterium tumefaciens* strain GV3101, and then the strains were transformed into *Arabidopsis* Col-0 plants with the floral-dip method [32].

2.6. Molecular Confirmation and Phenotypic Evaluation of Transgenic Plants

Transgenic lines were grown on half-strength MS agar medium supplied with 50 mg/L hygromycin, and then the positive transgenic plants were confirmed by RT-PCR detection. For RT-PCR, RNA from the leaves of transgenic lines and WT plants was isolated using the Trizol reagent (TianGen, Beijing, China) with the CsMADS26-specific primers (CsMADS26-3F: 5'-TTGGGAAAGGATCTCAC TGG-3', and CsMADS26-3R: 5'-CAGAGTTGCAGGCCATATCA-3'). The *AtTubulin4* gene was used as the reference gene, and the primers for the quantification were 5'-GCCAACAGTTCACAGCTATGTT CA-3' and 5'-GAGGGAGCCATTGACAACATCTT-3'. Positive T₃ homozygous seeds of at least two transgenic lines displaying 100% germination rate were selected for subsequent phenotypic evaluation.

3. Results and Discussion

3.1. Cloning and Sequence Analysis of CsMADS26

According to the locus ID of the CsMADS26 gene [28], we cloned its ORF by RT-PCR using specific primers from cucumber flowers. The amplification results showed that the ORF of CsMADS26 is 669 bp in length, and encodes a predicted protein of 222 amino acids, with a theoretical molecular weight (MW) of 25.36 kDa and a predicted isoelectric point of 5.57 (Figure 1). In addition, CsMADS26 has 36 negatively charged and 31 positively charged amino acids, with a putative grand average of

hydropathy index (GRAVY) of -0.494 , suggesting that CsMADS26 is highly hydrophilic. The domain analysis showed that CsMADS26 holds the M, I, K, and C domains (Figure 1), which is a typical characteristic of MIKC-type MADS-box proteins [1]. WoLF PSORT server analysis showed that the CsMADS26 protein is located in the nucleus. These results indicate that CsMADS26 is a MIKC-type MADS-box transcription factor.

```

1   ATGGGTCGAGGGAAGATTGAAATCAAAGGATTGAGAATGCTAATAGCAGACAAGTTACATTCTCGAAGAGACGA
   M G R G K I E I K R I E N A N S R Q V T F S K R R
76  GCTGGTTGCTTAAGAAGGCTCAAGAACTTGCTATTCTTTGTGATGCTGAAGTTGCTGTTATTATCTTCTCTAAT
   A G L L K K A Q E L A I L C D A E V A V I I F S N
151 ACTGGCAAGCTTTTCGAGTTTCTAGTTCTGGCATGAAGCACACTCTTGCAAGATACAACAAATGTGTAGAATCT
   T G K L F E F S S S G M K H T L A R Y N K C V E S
226 TCAGATGTACAGTAGACGTGACAAGTTGAGCGAGAGCATGAGGAGGTAGACATTCTACGAGAGGAAATAACA
   S D A T V D V H K V E R E H E E V D I L R E E I T
301 ACTCTGCAAAATGAAACAATTACAGCTATTGGGAAAGGATCTCACTGGCTTAGGCTTCAAAGAGTTGCAAAACCTG
   T L Q M K Q L Q L L G K D L T G L G F K E L Q N L
376 GAGCAACAGCTAAATGAAGGCTATTACTGGTAAAAGAGAAGAAGAACAGTTACTGATGGAGCACTAGAGCAA
   E Q Q L N E G L L L V K E K K E Q L L M E Q L E Q
451 TCAAGGTACAGGAACAACGAGCAATGCTTGAGAACGAAACTCTGCGGAGACAGGTCATGAGCTTCGGTGTCTG
   S R V Q E Q R A M L E N E T L R R Q V N E L R C L
526 TTTCCGCGGTTGATTGCCCTTCCAGCTTATCTTGAATACTGCTCCCTAGAGCAAAGAATATTGGCATTAGA
   F P P V D C P L P A Y L E Y C S L E Q K N I G I R
601 AGCCCTGATATGCCCTGCAACTCTGAAATGAAAAGGAGATTGAGACACCACCTTGCCTTGGGGTAA
   S P D M A C N S E I E R G D S D T T L H L G *
    
```

Figure 1. Nucleotide and predicted amino acid sequences of CsMADS26. Stop codon is marked by asterisk. The M, I, K, and C domains are underlined with red, green, pink, and blue lines, respectively.

The secondary structure of the CsMADS26 protein was predicted by SOPMA. As a result, CsMADS26 contains 55.86% alpha helices, 12.61% extended strands, 4.50% beta turns, and 27.03% random coils, respectively (Figure 2). Previous reports have suggested that the K domain is mainly responsible for dimerization [2,9]. However, CsMADS26 possesses a large number of alpha helices in its K domain, suggesting that CsMADS26 may have a particular function in facilitating the dimerization of MADS-box proteins. Interestingly, the C domain of CsMADS26 mainly contains random coils (Figure 2), which might contribute to the formation of protein complex and transcriptional activation [1,10].

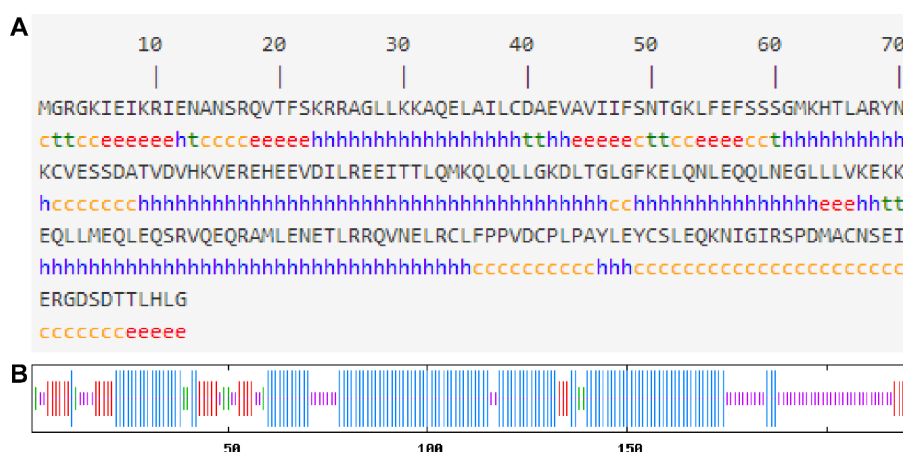


Figure 2. Secondary structure of CsMADS26 protein predicted by SOPMA. (A) Detailed amino acid information of CsMADS26 protein. The letters "c", "t", "e", and "h" represent random coil, beta turn, extended strand, and alpha helix, respectively. (B) Overview of the secondary structure of CsMADS26 protein. The blue longest lines, red lines, green lines, and purple shortest lines represent alpha helices, extended strands, beta turns, and random coils, respectively.

3.2. Sequence Alignment of CsMADS26 and Other AGL15 Subfamily Proteins

The results of multiple sequence alignment revealed that CsMADS26 shares high amino acid identities with other AGL15 subfamily proteins. For example, it showed 78.28%, 74.66%, 73.30%, 72.07%, 70.32%, 69.12%, 62.16%, and 60.95% sequence identity with HbAGL15, ZjMADS45, PpMADS14, MnMADS6, VvMADS25, RcAGL15, SIMBP11, and AtAGL15, respectively (Figure 3). The alignment results also showed that all of these proteins contain a highly conserved M domain in the N-terminus and a variable C domain in the C-terminus, while the I and K domains are less conserved (Figure 3). Additionally, the signature motif of AGL15 subfamily proteins, SD(T/I)TL(Q/H)LGL, is present in the C-domain of these proteins, with the exception of CsMADS26, which lacks the last “L” residue. The signature motif is also present in some other AGL15 subfamily proteins [18,23].

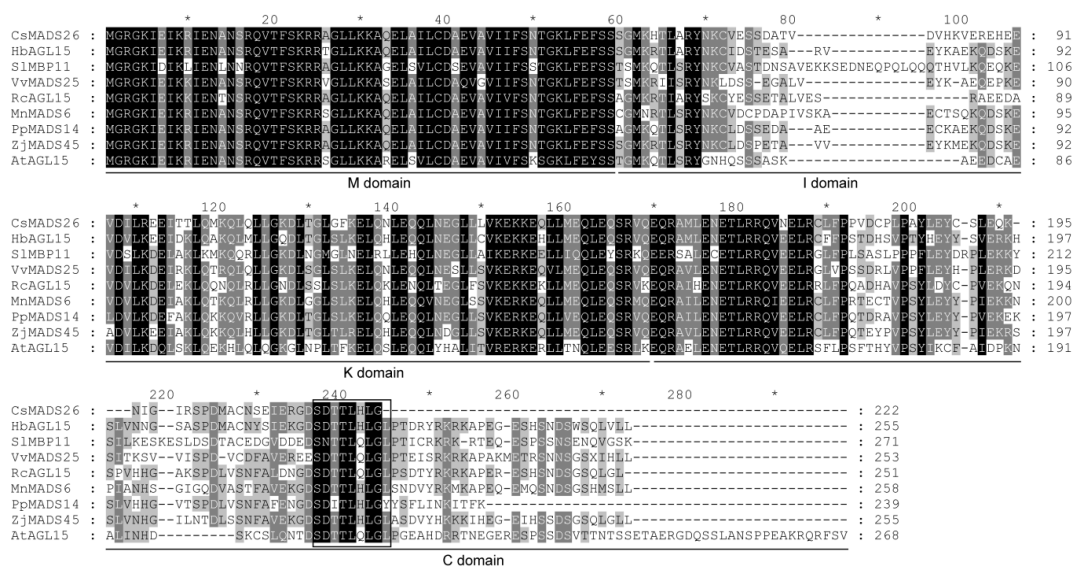


Figure 3. Sequence alignment of CsMADS26 and other AGL15 subfamily proteins. Multiple sequence alignment was performed by Clustal Omega using default settings with full-length amino acid sequences of these proteins. The M, I, K, and C domains are underlined. The signature sequences of AGL15 subfamily proteins are boxed. The AGL15 subfamily members used in the sequence alignment were obtained from Genbank, including AtAGL15 (*Arabidopsis thaliana*, At5g13790), RcAGL15 (*Rosa canina*, KM083102), SIMBP11 (*Solanum lycopersicum*, XM_004229626), PpMADS14 (*Prunus persica*, KU559580), VvMADS25 (*Vitis vinifera*, XM_003633492), ZjMADS45 (*Ziziphus jujuba*, XM_016026070.1), HbAGL15 (*Hevea brasiliensis*, KY471151), and MnMADS30 (*Morus notabilis*, EXC18224.1).

3.3. Analysis of the Molecular Evolution of CsMADS26

Our previous report has shown that CsMADS26 together with CsMADS25 belongs to the AGL15 subfamily of the MIKC^C-type MADS-box proteins [28]. To dissect the phylogenetic relationships of CsMADS26 and AGL15 subfamily members from other plant species, a phylogenetic tree was created using NJ method with the amino acid sequences. The results demonstrated that these AGL15 subfamily proteins could be divided into two clades: AGL15 clade and AGL18 clade (Figure 4), indicating that AGL15 and AGL18 proteins might have evolved from one common ancestor in plants [27]. CsMADS26 together with CmMADS08 and other AGL15 proteins were clustered in the AGL15 clade, whereas CsMADS25 was grouped into the AGL18 clade (Figure 4).

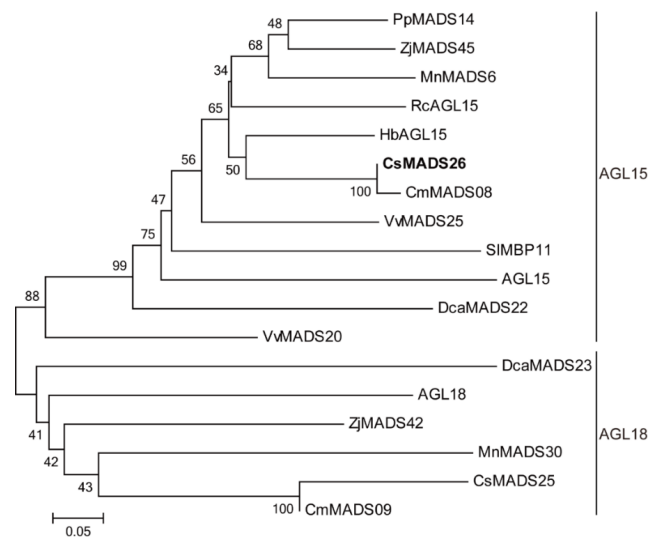


Figure 4. Phylogenetic relationships of *CsMADS26* and AGL15 subfamily members from other plant species. Sequence alignment was carried out by using Clustal Omega with protein sequences from various plant species, and the alignment results were used to generate a NJ phylogenetic tree by MEGA 5.0 software with 1000 bootstrap replicates. The information and relative references of these proteins are provided in Table S1.

3.4. Tissue Expression Profiles of *CsMADS26* in *Cucumber*

To evaluate the tissue expression profiles of *CsMADS26* in cucumber, we performed qRT-PCR to analyze the transcript accumulation of *CsMADS26* in different tissues, including male flower, female flower, root, stem, leaf, and fruit. As shown in Figure 5, the expression of *CsMADS26* was detected in the six tested tissues, with the highest levels in male flower and female flower, followed by fruit and leaf, and much lower levels in stem and root. *CsMADS26* is mainly expressed in reproductive organs, which is in agreement with the profiles of other AGL15 subfamily genes in various plants, including *Prunus mume* (*PmMADS30*) [33], *Vitis vinifera* (*VvMADS20* and *VvMADS25*) [34], *P. bretschneideri* (*PbrMADS34* and *PbrMADS37*) [9], *Z. jujuba* (*ZjMADS42* and *ZjMADS45*) [10], *G. hirsutum* (*GhAGL15-3*) [2], *D. caryophyllus* (*DcaMADS22* and *DcaMADS23*) [12], and *M. notabilis* (*MnMADS6*) [7], indicating its important function in the development of reproductive organs. In addition, its expression was also observed in leaf, indicating that *CsMADS26* might play a role in leaf development.

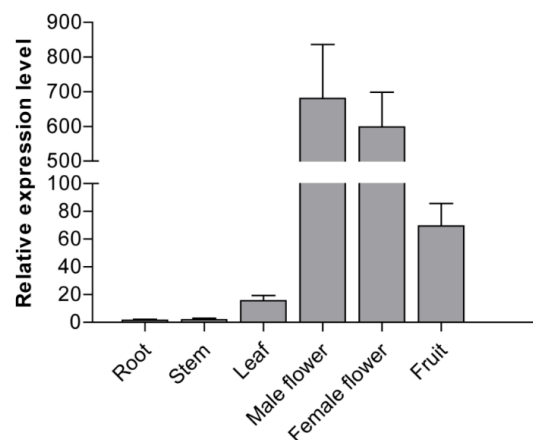


Figure 5. Expression profile analysis of *CsMADS26* in various tissues of cucumber by qRT-PCR. The value for root was set as one when calculating the relative expression levels of *CsMADS26* in other tissues. Data are presented as the mean values and standard deviation (SD) from three experimental replicates.

3.5. Abnormal Leaf Morphology Induced by *CsMADS26* Overexpression in *Arabidopsis*

To gain further insights into the function of *CsMADS26*, the ORF of *CsMADS26* was inserted into pHB vector for ectopic expression in *Arabidopsis* (Figure 6A). All of the 14 independent positive 35S::35S::*CsMADS26* transgenic plants displayed a phenotype of curled leaves, with 8 displaying a strong phenotype and 6 displaying a weak phenotype. In addition to curled leaves, no other phenotypes were observed in these positive transgenic plants. These transgenic lines were confirmed by RT-PCR analysis, and two lines (OE1 and OE2) were selected for further analysis (Figure 6B).

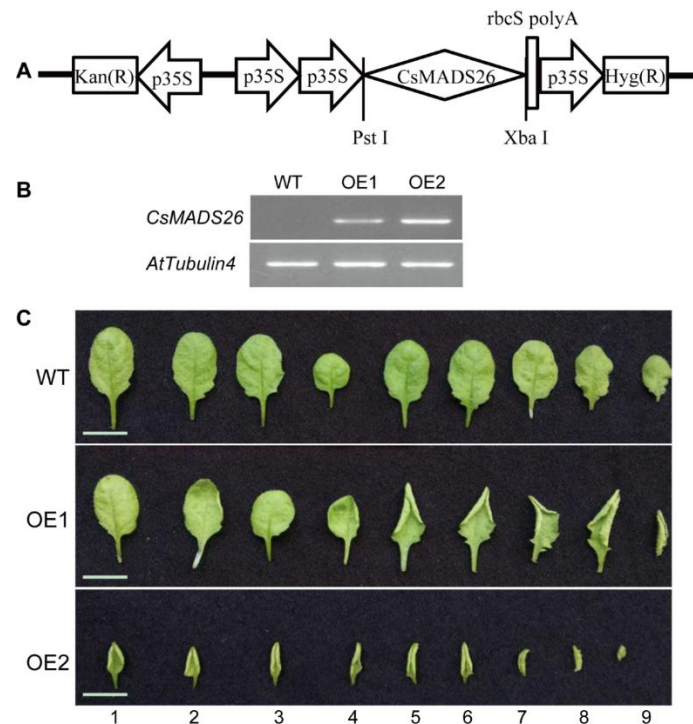


Figure 6. (A) Schematic diagram of 35S::35S::*CsMADS26* construct used for *Arabidopsis* transformation. (B) RT-PCR analysis of the expression of *CsMADS26* in WT and two transgenic lines (OE1 and OE2) by using the *AtTubulin4* gene as an internal control. (C) Morphology of the rosette leaves in WT and transgenic plants (OE1 and OE2) under long-day conditions. The leaves were separated from 20-day-old plants. Bar = 1 cm.

To further analyze the phenotype of curled leaves, we compared all the nine rosette leaves between WT and transgenic *Arabidopsis* plants. Compared with the WT plants, the 1st to 4th leaves of the transgenic line with low *CsMADS26* expression (OE1) showed no significant phenotype of curled leaves, while the 5th to 9th leaves of OE1 exhibited an upward curling of the leaf margins (Figure 6C); in the transgenic line with high *CsMADS26* expression (OE2), all of the leaves were severely curled, and the curling degree was much higher than that in OE1 and WT plants, suggesting that the curling of leaves may be due to the overexpression of *CsMADS26* in *Arabidopsis*. Similar to *AtAGL15*, the high expression of *CsMADS26* in *Arabidopsis* may cause a decline in the expression of *miR156* to regulate *miR156*-mediated target gene expression, including *AtAGL15* and *AtAGL18* [15]. *agl15 agl18 agl24 svp* mutations also resulted in upward curling of rosette and cauline leaves under long-day conditions, and the leaf curling is related to the expression of genes that are involved in floral organ development, such as *SEP3* [16]. It is noteworthy that the number of rosette leaves and flowering time were not altered in transgenic plants, suggesting that *CsMADS26* is not involved in regulating floral transition, which is different from the role of *AtAGL15* [14]. In addition, the leaf size (length and width) of OE2 was much smaller than that of WT plants (Figure 6C). Similarly, overexpression of an *AGL15* ortholog (*SIMBP11*) in tomato also caused decreases in the length and width of leaves [35]. Therefore, *CsMADS26* may

function in cucumber leaf development by interacting with its target genes expressed in leaves or through MADS protein dimerization.

4. Conclusions

In this study, we cloned the *CsMADS26* gene from cucumber. Sequence and phylogenetic analysis showed that *CsMADS26* is a MADS-box transcription factor and has a close relationship with AGL15 clade proteins of the AGL15 subfamily. *CsMADS26* is mainly expressed in reproductive organs such as flowers and fruits. Ectopic expression of *CsMADS26* could result in an abnormal leaf morphology including curled and small leaves in *Arabidopsis*. These results suggest the important role of *CsMADS26* in regulating leaf development of cucumber.

Supplementary Materials: The following are available online at <http://www.mdpi.com/2073-4395/8/11/265/s1>. Table S1: The names and accession numbers of AGL15 subfamily proteins used for phylogenetic relationship analysis.

Author Contributions: data curation, Y.Z. and L.G.; funding acquisition, S.L.; methodology, L.G.; software, Y.Z. and L.H.; writing (original draft), Y.Z.; writing (review and editing), L.H., Y.Y. and S.L.

Funding: This research was funded by the Key Project of Youth Science Foundation of Jiangxi Province, grant number [20171ACB21025], and the National Natural Science Foundation of China, grant numbers [31460522 and 31660578].

Conflicts of Interest: The authors declare no conflict of interest.

References

1. Kaufmann, K.; Melzer, R.; Theissen, G. MIKC-type MADS-domain proteins: Structural modularity, protein interactions and network evolution in land plants. *Gene* **2005**, *347*, 183–198. [CrossRef] [PubMed]
2. Ren, Z.; Yu, D.; Yang, Z.; Li, C.; Qanmber, G.; Li, Y.; Li, J.; Liu, Z.; Lu, L.; Wang, L.; et al. Genome-wide identification of the MIKC-type MADS-box gene family in *Gossypium hirsutum* L. unravels their roles in flowering. *Front. Plant Sci.* **2017**, *8*, 384. [CrossRef] [PubMed]
3. Smaczniak, C.; Immink, R.G.; Angenent, G.C.; Kaufmann, K. Developmental and evolutionary diversity of plant MADS-domain factors: Insights from recent studies. *Development* **2012**, *139*, 3081–3098. [CrossRef] [PubMed]
4. Henschel, K.; Kofuji, R.; Hasebe, M.; Saedler, H.; Münster, T.; Theissen, G. Two ancient classes of MIKC-type MADS-box genes are present in the moss *Physcomitrella patens*. *Mol. Biol. Evol.* **2002**, *19*, 801–814. [CrossRef] [PubMed]
5. Li, H.F.; Dong, Q.L.; Li, G.X.; Ran, K. Identification and expression analysis of 11 MADS-box genes in peach (*Prunus persica* var. *nectarina* ‘Luxing’). *J. Hortic. Sci. Biotechnol.* **2018**, *93*, 232–243. [CrossRef]
6. Hao, X.; Fu, Y.; Zhao, W.; Liu, L.; Bade, R.; Hasi, A.; Hao, J. Genome-wide identification and analysis of the MADS-box gene family in melon. *J. Am. Soc. Hortic. Sci.* **2016**, *141*, 507–519. [CrossRef]
7. Luo, Y.; Li, H.; Xiang, Z.; He, N. Identification of *Morus notabilis* MADS-box genes and elucidation of the roles of *MnMADS33* during endodormancy. *Sci. Rep.* **2018**, *8*, 5860. [CrossRef] [PubMed]
8. Liu, J.; Zhang, J.; Zhang, J.; Miao, H.; Wang, J.; Gao, P.; Hu, W.; Jia, C.; Wang, Z.; Xu, B.; et al. Genome-wide analysis of banana MADS-box family closely related to fruit development and ripening. *Sci. Rep.* **2017**, *7*, 3467. [CrossRef] [PubMed]
9. Wang, R.; Ming, M.; Li, J.; Shi, D.; Qiao, X.; Li, L.; Zhang, S.; Wu, J. Genome-wide identification of the MADS-box transcription factor family in pear (*Pyrus bretschneideri*) reveals evolution and functional divergence. *PeerJ* **2017**, *5*, e3776. [CrossRef] [PubMed]
10. Zhang, L.; Zhao, J.; Feng, C.; Liu, M.; Wang, J.; Hu, Y. Genome-wide identification, characterization of the MADS-box gene family in Chinese jujube and their involvement in flower development. *Sci. Rep.* **2017**, *7*, 1025. [CrossRef] [PubMed]
11. Nardeli, S.M.; Artico, S.; Aoyagi, G.M.; de Moura, S.M.; da Franca Silva, T.; Grossi-de-Sa, M.F.; Romanel, E.; Alves-Ferreira, M. Genome-wide analysis of the MADS-box gene family in polyploid cotton (*Gossypium hirsutum*) and in its diploid parental species (*Gossypium arboreum* and *Gossypium raimondii*). *Plant Physiol. Biochem.* **2018**, *127*, 169–184. [CrossRef] [PubMed]

12. Zhang, X.; Wang, Q.; Yang, S.; Lin, S.; Bao, M.; Bendahmane, M.; Wu, Q.; Wang, C.; Fu, X. Identification and characterization of the MADS-box genes and their contribution to flower organ in carnation (*Dianthus caryophyllus* L.). *Genes* **2018**, *9*, 193. [[CrossRef](#)] [[PubMed](#)]
13. Wei, M.; Wang, Y.; Pan, R.; Li, W. Genome-wide identification and characterization of MADS-box family genes related to floral organ development and stress resistance in *Hevea brasiliensis* Müll. Arg. *Forests* **2018**, *9*, 304. [[CrossRef](#)]
14. Adamczyk, B.J.; Lehti-Shiu, M.D.; Fernandez, D.E. The MADS domain factors AGL15 and AGL18 act redundantly as repressors of the floral transition in Arabidopsis. *Plant J.* **2007**, *50*, 1007–1019. [[CrossRef](#)] [[PubMed](#)]
15. Serivichyaswat, P.; Ryu, H.S.; Kim, W.; Kim, S.; Chung, K.S.; Kim, J.J.; Ahn, J.H. Expression of the floral repressor miRNA156 is positively regulated by the AGAMOUS-like proteins AGL15 and AGL18. *Mol. Cells* **2015**, *38*, 259–266. [[CrossRef](#)] [[PubMed](#)]
16. Fernandez, D.E.; Wang, C.-T.; Zheng, Y.; Adamczyk, B.J.; Singhal, R.; Hall, P.K.; Perry, S.E. The MADS-domain factors AGAMOUS-LIKE15 and AGAMOUS-LIKE18, along with SHORT VEGETATIVE PHASE and AGAMOUS-LIKE24, are necessary to block floral gene expression during the vegetative phase. *Plant Physiol.* **2014**, *165*, 1591–1603. [[CrossRef](#)] [[PubMed](#)]
17. Fernandez, D.E.; Heck, G.R.; Perry, S.E.; Patterson, S.E.; Bleecker, A.B.; Fang, S.C. The embryo MADS domain factor AGL15 acts postembryonically: Inhibition of perianth senescence and abscission *via* constitutive expression. *Plant Cell* **2000**, *12*, 183–198. [[CrossRef](#)] [[PubMed](#)]
18. Yang, Z.; Li, C.; Wang, Y.; Zhang, C.; Wu, Z.; Zhang, X.; Liu, C.; Li, F. *GhAGL15s*, preferentially expressed during somatic embryogenesis, promote embryogenic callus formation in cotton (*Gossypium hirsutum* L.). *Mol. Genet. Genomics* **2014**, *289*, 873–883. [[CrossRef](#)] [[PubMed](#)]
19. Zheng, Q.; Zheng, Y.; Ji, H.; Burnie, W.; Perry, S.E. Gene regulation by the AGL15 transcription factor reveals hormone interactions in somatic embryogenesis. *Plant Physiol.* **2016**, *172*, 2374–2387. [[CrossRef](#)] [[PubMed](#)]
20. Zheng, Q.; Zheng, Y.; Perry, S.E. AGAMOUS-Like15 promotes somatic embryogenesis in Arabidopsis and soybean in part by the control of ethylene biosynthesis and response. *Plant Physiol.* **2013**, *161*, 2113–2127. [[CrossRef](#)] [[PubMed](#)]
21. Zheng, Q.; Perry, S.E. Alterations in the transcriptome of soybean in response to enhanced somatic embryogenesis promoted by orthologs of AGAMOUS-Like15 and AGAMOUS-Like18. *Plant Physiol.* **2014**, *164*, 1365–1377. [[CrossRef](#)] [[PubMed](#)]
22. Xu, K.; Liu, K.; Wu, J.; Wang, W.; Zhu, Y.; Li, C.; Zhao, M.; Wang, Y.; Li, C.; Zhao, L. A MADS-box gene associated with protocorm-like body formation in *Rosa canina* alters floral organ development in Arabidopsis. *Can. J. Plant Sci.* **2018**, *98*, 309–317. [[CrossRef](#)]
23. Li, C.; Ma, G.; Xie, T.; Chen, J.; Wang, Z.; Song, M.; Tang, Q. *SOC1* and *AGL24* interact with *AGL18-1*, not the other family members *AGL18-2* and *AGL18-3* in *Brassica juncea*. *Acta Physiol. Plant.* **2018**, *40*, 3. [[CrossRef](#)]
24. Wang, H.; Caruso, L.V.; Downie, A.B.; Perry, S.E. The embryo MADS domain protein AGAMOUS-Like 15 directly regulates expression of a gene encoding an enzyme involved in gibberellin metabolism. *Plant Cell* **2004**, *16*, 1206–1219. [[CrossRef](#)] [[PubMed](#)]
25. Zheng, Y.; Ren, N.; Wang, H.; Stromberg, A.J.; Perry, S.E. Global identification of targets of the Arabidopsis MADS domain protein AGAMOUS-Like15. *Plant Cell* **2009**, *21*, 2563–2577. [[CrossRef](#)] [[PubMed](#)]
26. Zhou, Y.; Hu, L.; Ge, L.; Li, G.; He, P.; Jiang, L.; Liu, S. Ectopic expression of *CsMADS24*, an AGAMOUS ortholog from cucumber, causes a homeotic conversion of sepals into carpels in transgenic Arabidopsis plants. *Arch. Biol. Sci.* **2018**. [[CrossRef](#)]
27. Zhou, Y.; Hu, L.; Ge, L.; He, P.; Yang, Y.; Liu, S. Isolation and functional characterization of an AGAMOUS-LIKE 18 (*AGL18*) MADS-box gene from cucumber (*Cucumis sativus* L.). *Not. Bot. Horti Agrobot.* **2019**. [[CrossRef](#)]
28. Hu, L.; Liu, S. Genome-wide analysis of the MADS-box gene family in cucumber. *Genome* **2012**, *55*, 245–256. [[CrossRef](#)] [[PubMed](#)]
29. Geourjon, C.; Deleage, G. SOPMA: Significant improvements in protein secondary structure prediction by consensus prediction from multiple alignments. *Bioinformatics* **1995**, *11*, 681–684. [[CrossRef](#)]
30. Sievers, F.; Wilm, A.; Dineen, D.; Gibson, T.J.; Karplus, K.; Li, W.; Lopez, R.; McWilliam, H.; Remmert, M.; Soding, J.; et al. Fast, scalable generation of high-quality protein multiple sequence alignments using Clustal Omega. *Mol. Syst. Biol.* **2011**, *7*, 539. [[CrossRef](#)] [[PubMed](#)]

31. Livak, K.J.; Schmittgen, T.D. Analysis of relative gene expression data using real-time quantitative PCR and the $2^{-\Delta\Delta C_t}$ method. *Methods* **2001**, *25*, 402–408. [[CrossRef](#)] [[PubMed](#)]
32. Clough, S.J.; Bent, A.F. Floral dip: A simplified method for *Agrobacterium*-mediated transformation of *Arabidopsis thaliana*. *Plant J.* **1998**, *16*, 735–743. [[CrossRef](#)] [[PubMed](#)]
33. Xu, Z.; Zhang, Q.; Sun, L.; Du, D.; Cheng, T.; Pan, H.; Yang, W.; Wang, J. Genome-wide identification, characterisation and expression analysis of the MADS-box gene family in *Prunus mume*. *Mol. Genet. Genomics* **2014**, *289*, 903–920. [[CrossRef](#)] [[PubMed](#)]
34. Wang, L.; Yin, X.; Cheng, C.; Wang, H.; Guo, R.; Xu, X.; Zhao, J.; Zheng, Y.; Wang, X. Evolutionary and expression analysis of a MADS-box gene superfamily involved in ovule development of seeded and seedless grapevines. *Mol. Genet. Genomics* **2015**, *290*, 825–846. [[CrossRef](#)] [[PubMed](#)]
35. Guo, X.; Chen, G.; Naeem, M.; Yu, X.; Tang, B.; Li, A.; Hu, Z. The MADS-box gene *SIMBP11* regulates plant architecture and affects reproductive development in tomato plants. *Plant Sci.* **2017**, *258*, 90–101. [[CrossRef](#)] [[PubMed](#)]



© 2018 by the authors. Licensee MDPI, Basel, Switzerland. This article is an open access article distributed under the terms and conditions of the Creative Commons Attribution (CC BY) license (<http://creativecommons.org/licenses/by/4.0/>).